JOINT INSTITUTE FOR NUCLEAR RESEARCH

2006-184

M. G. Itkis

FLEROV LABORATORY OF NUCLEAR REACTIONS

RESEARCH ACTIVITIES IN 2006

Report to the 101st Session
of the JINR Scientific Council
January 18–19, 2007

Dubna 2006

M. G. Itkis

FLEROV LABORATORY OF NUCLEAR REACTIONS

RESEARCH ACTIVITIES IN 2006

Report to the 101st Session
of the JINR Scientific Council
January 18–19, 2007

Dubna 2006

In 2006, the FLNR scientific program on heavy ion physics included experiments on the synthesis of heavy and exotic nuclei using ion beams of stable and radioactive isotopes and studies of nuclear reactions, acceleration technology, heavy ion interaction with matter, and applied research. These lines of investigations were represented in 3 laboratory topics and 1 all-institute project:

- Synthesis of new nuclei and study of nuclear properties and heavy ion reaction mechanisms (12 subtopics);
- Radiation effects and modification of materials, radioanalytical and radioisotopic investigations using the FLNR accelerators (5 subtopisc);
- Development of the FLNR cyclotron complex for producing intense beams of accelerated ions of stable and radioactive isotopes (2 subtopics);
- Development of the U400+U400M+MT25 cyclotron-microtron complex for the production of radioactive ion beams (the DRIBs project, 4 subtopics).

In 2006, the operation time of the U400 and U400M FLNR cyclotrons was nearly 9000 hours, which is in accordance with the plan. Due to this, new experiments in low and medium energy ranges were possible.

Synthesis of new elements

In experiments performed in 1999-2005, 17 new heaviest nuclides with Z=112-116 and 118 as well as their daughter isotopes of lighter elements have been produced in the complete-fusion reactions of ^{238}U, ^{242,244}Pu, ^{243}Am, ^{245,248}Cm and ^{249}Cf targets with ^{48}Ca beams [1]. While sequences of four neighboring isotopes of each of even-Z elements 112, 114 and 116, i.e., $^{282-285}$112, $^{286-289}$114 and $^{290-293}$116 were observed in various cross bombardments, for odd-Z elements only pairs of isotopes ^{283,284}113 and ^{287,288}115 were synthesized in a single reaction ^{243}Am+^{48}Ca.

This year we further continued investigation of the new region of enhanced nuclear stability of the superheavy nuclei by synthesizing isotopes of element 113 direct in the reaction ^{237}Np+^{48}Ca [2]. The synthesis of the neighboring lighter isotopes of element 113 and their α-decay daughters in the ^{237}Np(^{48}Ca,xn)$^{285-x}$113 reaction could provide valuable information concerning influence of the neutron shells at N=162 and N=184 on the pattern of changes of the decay properties of nuclei depending on the neutron number at the edge of the region of spherical superheavy nuclides. Moreover, the ^{237}Np+^{48}Ca reaction results in a compound nucleus ^{285}113 which is two α particles lighter than ^{293}117, the product of the complete-fusion reaction ^{243}Am+^{50}Ti, that could be used further for the synthesis of the still unknown element 117.

Irradiation of the ^{237}Np (>99%, 0.37 mg/cm^2) target by ^{48}Ca projectiles was performed in June-July 2006 using the Dubna gas-filled recoil separator. The total beam dose of ^{48}Ca-ions of 1.1×10^{19} was accumulated. The lab-frame projectile energy in the middle of the target layer was 244 MeV that corresponds to the excitation-energy interval of compound nuclei ^{285}113 of 39.1±2.2 MeV.

In the ^{237}Np+^{48}Ca reaction two decay chains of new isotope ^{282}113 were observed for the first time. The decay properties of four α-decaying isotopes ^{282}113 (E_α=10.63±0.08 MeV, $T_{1/2}=73^{+134}_{-29}$ ms), ^{278}Rg (E_α=10.69±0.08 MeV, $T_{1/2}=4.2^{+7.5}_{-1.7}$ ms), ^{274}Mt (E_α=10.0±1.1 and 9.76±0.10 MeV, $T_{1/2}=440^{+810}_{-170}$ ms), and ^{270}Bh (E_α=8.93±0.08 MeV, $T_{1/2}=61^{+292}_{-28}$ s) were determined. We suppose that the terminal nucleus ^{266}Db most probably undergoes electron capture with a half-life of 22^{+105}_{-10} min followed by relatively short spontaneous fission of the even-even isotope ^{266}Rf (T_{SF}≈20 s is predicted).

The production cross section of the 3*n*-evaporation channel of the reaction was measured to be about 1 pb.

Atomic and mass numbers of the isotope of element 113 were determined from the comparison of measured cross section and decay characteristics of observed nuclei with theoretical predictions and systematics of experimental data (see Fig. 1).

The production cross section of element 113 in the reaction ^{237}Np+^{48}Ca exceeds that of the lighter isotope of element 113 synthesized in the cold fusion reaction ^{209}Bi+^{70}Zn by more than an order of magnitude. The decay properties of five new isotopes with *Z*=105-113 and their production cross section in the reaction of ^{237}Np with ^{48}Ca are in agreement with the modern concepts of the influence of nuclear shells on the stability of heavy and superheavy nuclei.

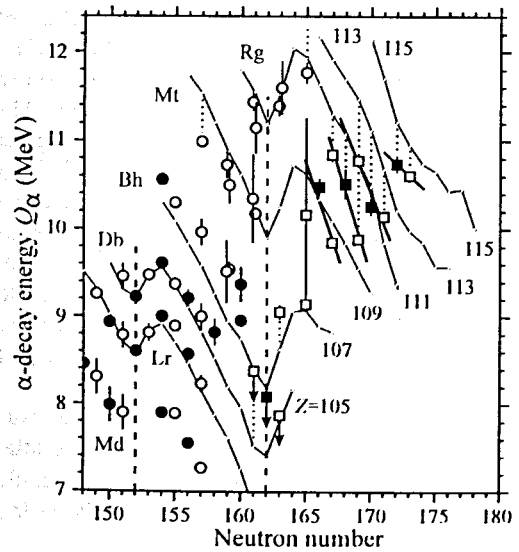

Fig. 1. α-decay energy *vs.* neutron number for odd-*Z* elements Md through 115 (solid and open symbols – even-*N* and odd-*N* isotopes, respectively, squares – data from ^{48}Ca-induced reactions). The values shown for ^{266,267,268}Db isotopes are the upper limits, since α emission of these nuclides has not been observed. Small open symbols connected by lines show the theoretical Q_α values calculated for the same isotopes in the macroscopic-microscopic model.

Chemistry of transactinides and the separator MASHA

Chemistry of Db. In December 2005 a joint chemical experiment with the group from LLNL, USA was performed [3]. The goal of the experiment was to continue studying the chemical properties of element Db that was produced as a progeny of ^{288}115 in the reaction ^{243}Am + ^{48}Ca.

The June 2004 chemistry experiment provided evidence that the spontaneously-fissioning species was ^{268}Db since the fissions occurred in the fraction that contained the +5 species. However there was a significant amount of +4 species also in that fraction, so an additional chemical separation was desired.

Chemical separation of the +4 and +5 species was needed to further narrow down the elemental identification of the spontaneously-fissioning species. It was also considered creating Nb-like and Ta-like fractions from the +5 species to begin determining if Db behaves more like Nb or Ta under these chemical conditions.

With these two ideas in mind FLNR and LLNL chemists set about creating a separation scheme to use for the next experiment in December 2005. Each group developed a chemical procedure: FLNR's procedure was based on anion exchange chromatography and LLNL's procedure was based on reverse phase chromatography. The experimental set up for the December 2005 chemistry experiment was similar to the set up in June 2004.

A total of eight irradiations with average beam integral 4.5×10^{17}were performed at the FLNR cyclotron U400. For two of the irradiations the LLNL procedure was used and for the other six irradiations the FLNR procedure.

For three of the irradiations, a +4 fraction was generated in addition to the +5 fractions. From five of the irradiations a spontaneous fission was observed in a counting sample. All of the spontaneous fissions were observed in a +5 fraction, three of the +5 fractions had been further partitioned into Nb and Ta and in each of these cases the spontaneous fission occurred in the Ta fraction.

Unfortunately the samples produced were thicker then in previous experiment which resulted in rather low spontaneous fission energies (the fission fragments observed ranged from 3 to 66 MeV, they are obviously spontaneous fissions since all were accompanied by at least 1 neutron).

Chemistry of Element 112. In April-May 2006 a joint chemical experiment with the group from PSI, Switzerland was performed [4].

Element 112 is a representative of group 12 together with zinc, cadmium, and mercury and has a filled electron configuration [Rn] $5f^{14}6d^{10}7s^2$. Thus, a noble metallic character can be expected. However, relativistic calculations of atomic properties of superheavy elements (SHE) suggest the contraction of the spherical s- and $p_{1/2}$- electron orbitals. This may lead to an increased chemical stability of the elemental atomic state for element 112. Early predictions for element 112 reach from mercury-like behaviour to radon-like inertness.

As the result of the experiment first chemical properties were measured for element 112. The isotope ^{283}112 was produced in the nuclear fusion reaction of ^{48}Ca with ^{242}Pu and the subsequent alpha decay of the short-lived ^{287}114. The target

of ^{242}Pu (1400 μg/cm^2) with an admixture of $^{nat.}$Nd (50 μg/cm^2), which was prepared on Ti foils, was irradiated for a time period of about 3 weeks at the U400 cyclotron of FLNR. The beam energy in the middle of the target was 236±3 MeV, thus producing ^{287}114 in the reaction ^{242}Pu(^{48}Ca,3n). Simultaneously, the α-decaying nuclide ^{185}Hg having a half-life of 49 s was produced in the reaction ^{142}Nd(^{48}Ca, 5n). Various isotopes of radon (e.g., ^{219}Rn, with a half-life of 3.96 s) were produced in multinucleon transfer reactions. Radon and mercury were studied simultaneously with element 112 throughout the entire experiment.

The nuclear reaction products were thermalized in a recoil chamber flushed by the carrier gas He/Ar mixture. The separation technique guaranteed that only volatile nuclear reaction products were transported through a capillary of 8 m length to the detection system. An average transport time of about 3.6 s was measured using ^{185}Hg.

The detection system Cryo-On-Line Detector (COLD) consists of an array of 32 pairs of PIPS-detectors, which were combined with the active surfaces facing each other, forming a rectangular channel with an open cross section of 9.7 x 1.6 mm^2. The surface of the detectors on one side of the channel was covered by a 50 nm gold layer. The temperature gradient was established along this chromatographic channel by a thermostat heating at the inlet and a liquid-nitrogen cryostat cooling near the outlet. The event-by-event spectroscopy with the PIPS detectors provided an on-line identification of spontaneously fissioning and α-decaying nuclides that were deposited on the detector's surfaces.

During the three-weeks experiment two genetically linked decay chains were detected and unambiguously attributed to the decay of ^{283}112 (Fig. 2).

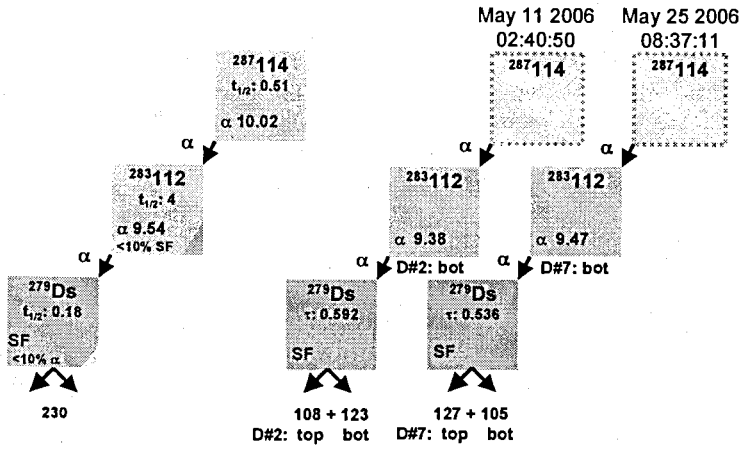

Fig. 2. The two decay chains observed in the COLD thermochromatography detector and attributed to the decay of ^{283}112 are shown on the right side in comparison to the reported earlier decay properties of ^{283}112 on the left side.

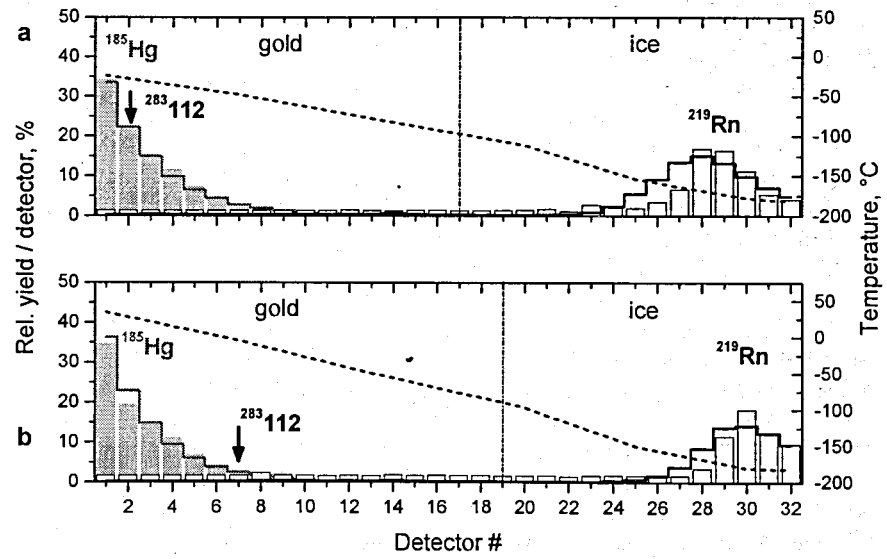

Fig. 3 Results of thermochromatographic separations of element 112 compared to mercury and radon in the COLD detector.

The primary product, ^{287}114, having a half-life of about 0.5 s is too short-lived to be transported to the COLD detector. Therefore, only decay of the daughter nuclei ^{283}112 and ^{279}Ds could be detected.

In the first part of the experiment run the inlet of the detector array was held at -30°C to reach the lowest possible temperature of -184°C at the cold end of the detector. The measured distribution of ^{185}Hg, ^{219}Rn, and ^{283}112 along the detector array is presented in Fig. 3a. Indeed about 88% of the ^{219}Rn deposited on the last 8 detectors. A deposition of ^{185}Hg on the gold surface was observed within in the first eight detectors (Fig. 3a). At these conditions the first atom of ^{283}112 was detected on the second detector at a temperature of -28°C (Fig. 3a, black arrow). This observation allows for the determination of only a lower limit of $-\Delta H_{ads}^{Au}(E112) > 47$ kJ/mol.

In the second run the temperature at the inlet of the detectors was increased up to 35°C. Accordingly, a temperature of -180°C was achieved at the cold end of the thermochromatography channel (Fig. 3b). At these new conditions about 53 % of the ^{219}Rn deposited on the last five detectors. The observed second atom of ^{283}112 deposited on the seventh detector held at -5°C. (Fig. 3b).

From the observation of both atoms of element 112 the statistical Monte Carlo approach of gas chromatography allows to quantify the interaction of element 112 with Au as $-\Delta H_{ads}^{Au}(E112) = 52^{+46}_{-7}$ kJ/mol. We conclude that a metal-metal bond formation is involved into the adsorption interaction of element 112 with gold. This is typical group 12 element behaviour.

of ^{242}Pu (1400 μg/cm^2) with an admixture of ^{nat}Nd (50 μg/cm^2), which was prepared on Ti foils, was irradiated for a time period of about 3 weeks at the U400 cyclotron of FLNR. The beam energy in the middle of the target was 236±3 MeV, thus producing ^{287}114 in the reaction ^{242}Pu(^{48}Ca,3n). Simultaneously, the α-decaying nuclide ^{185}Hg having a half-life of 49 s was produced in the reaction ^{142}Nd(^{48}Ca, 5n). Various isotopes of radon (e.g., ^{219}Rn, with a half-life of 3.96 s) were produced in multinucleon transfer reactions. Radon and mercury were studied simultaneously with element 112 throughout the entire experiment.

The nuclear reaction products were thermalized in a recoil chamber flushed by the carrier gas He/Ar mixture. The separation technique guaranteed that only volatile nuclear reaction products were transported through a capillary of 8 m length to the detection system. An average transport time of about 3.6 s was measured using ^{185}Hg.

The detection system Cryo-On-Line Detector (COLD) consists of an array of 32 pairs of PIPS-detectors, which were combined with the active surfaces facing each other, forming a rectangular channel with an open cross section of 9.7 x 1.6 mm^2. The surface of the detectors on one side of the channel was covered by a 50 nm gold layer. The temperature gradient was established along this chromatographic channel by a thermostat heating at the inlet and a liquid-nitrogen cryostat cooling near the outlet. The event-by-event spectroscopy with the PIPS detectors provided an on-line identification of spontaneously fissioning and α-decaying nuclides that were deposited on the detector's surfaces.

During the three-weeks experiment two genetically linked decay chains were detected and unambiguously attributed to the decay of ^{283}112 (Fig. 2).

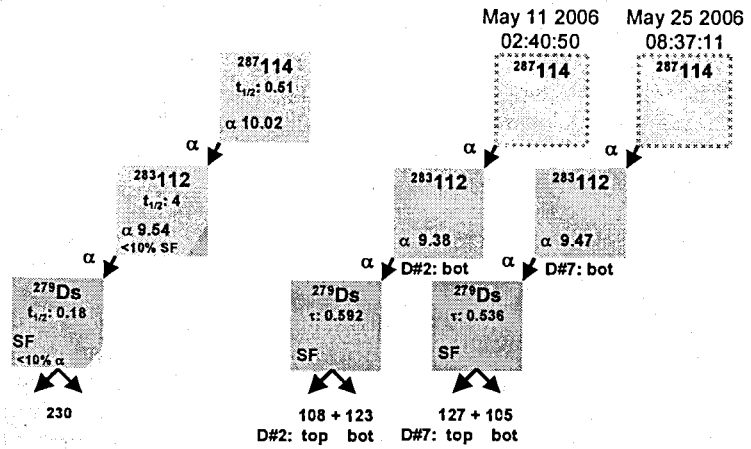

Fig. 2. The two decay chains observed in the COLD thermochromatography detector and attributed to the decay of ^{283}112 are shown on the right side in comparison to the reported earlier decay properties of ^{283}112 on the left side.

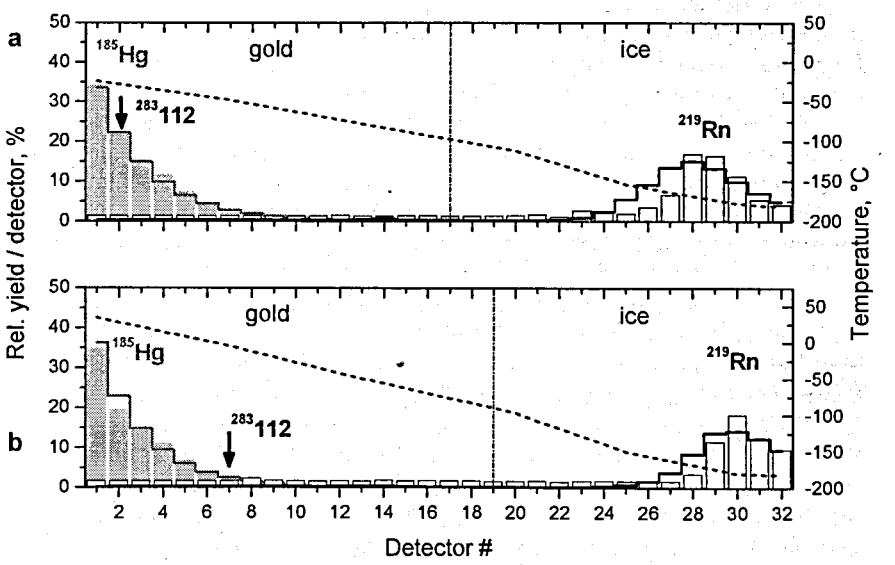

Fig. 3 Results of thermochromatographic separations of element 112 compared to mercury and radon in the COLD detector.

The primary product, ^{287}114, having a half-life of about 0.5 s is too short-lived to be transported to the COLD detector. Therefore, only decay of the daughter nuclei ^{283}112 and ^{279}Ds could be detected.

In the first part of the experiment run the inlet of the detector array was held at -30°C to reach the lowest possible temperature of -184°C at the cold end of the detector. The measured distribution of ^{185}Hg, ^{219}Rn, and ^{283}112 along the detector array is presented in Fig. 3a. Indeed about 88% of the ^{219}Rn deposited on the last 8 detectors. A deposition of ^{185}Hg on the gold surface was observed within in the first eight detectors (Fig. 3a). At these conditions the first atom of ^{283}112 was detected on the second detector at a temperature of -28°C (Fig. 3a, black arrow). This observation allows for the determination of only a lower limit of $-\Delta H_{ads}^{Au}(E112) > 47$ kJ/mol.

In the second run the temperature at the inlet of the detectors was increased up to 35°C. Accordingly, a temperature of -180°C was achieved at the cold end of the thermochromatography channel (Fig. 3b). At these new conditions about 53 % of the ^{219}Rn deposited on the last five detectors. The observed second atom of ^{283}112 deposited on the seventh detector held at -5°C. (Fig. 3b).

From the observation of both atoms of element 112 the statistical Monte Carlo approach of gas chromatography allows to quantify the interaction of element 112 with Au as $-\Delta H_{ads}^{Au}(E112) = 52^{+46}_{-7}$ kJ/mol. We conclude that a metal-metal bond formation is involved into the adsorption interaction of element 112 with gold. This is typical group 12 element behaviour.

The observed two SF decays of ^{279}Ds were the only SF events measured throughout the experiment. The coincident detection of both high energetic SF fragments revealed a total kinetic energy of about 230 MeV, which is typical for the SF decay of a very heavy nucleus. The correlation of both observed SF events to a 9.43±0.1 MeV alpha decay within the preceding 0.5 s in the same detector renders this decay pattern completely free of background. The detected decays agree with the decay properties reported from the experiments in 2004 at FLNR.

Thus, this observation represents a first independent and unambiguous confirmation of the formation of element 112 in the fusion reaction of ^{48}Ca with ^{242}Pu. The primary product, ^{287}114, having a half-life of about 0.5 s is too short-lived to be transported to the COLD detector. Therefore, only ^{283}112 and ^{279}Ds could be detected. A lower limit lifetime of about 2 s can be estimated for ^{283}112.

Mass measurements of ^{268}Db. To confirm the mass assignment of the Db isotope it is planned to determine the mass of that nuclei at the FLNR mass analyzer of super heavy atoms MASHA. The initial compounds for introduction into the MASHA ECR ion source should be volatile. A method of selective and quantitative transfer of anionic fluoride complexes of the group 5 elements into volatile pentafluorides using XeF_2 as a fluorinating agent was developed. Model tests showed that almost 100% of TaF_5 leave the feeding tube.

Nuclear fission

The experiment on the study of the fusion-fission process of the element ^{294}116 in the reactions ^{48}Ca +^{246}Cm and ^{50}Ti + ^{244}Pu was carried out in FLNR JINR with use of double arm time-of-flight position-sensitive spectrometer CORSET [5]. The mass-energy distributions of the fragments and the excitation functions for these reactions were obtained (Fig. 4).

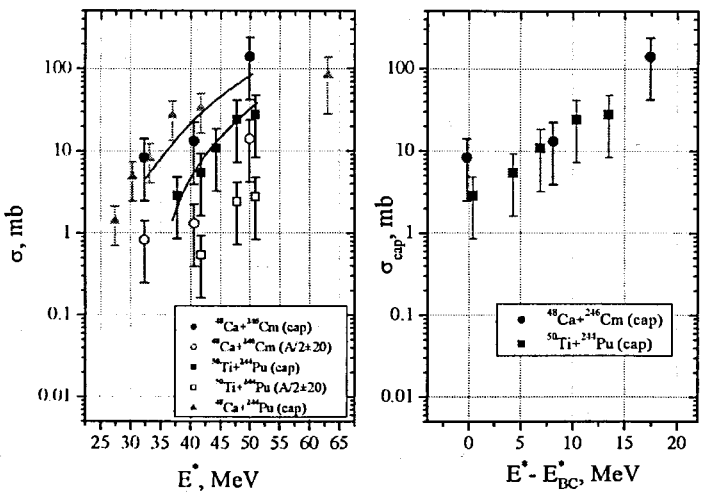

Fig. 4. Capture cross sections for the reactions ^{50}Ti+^{244}Pu and ^{48}Ca+^{246}Cm

The heaviest element, which can be obtained with ^{48}Ca-ions, is the nucleus with Z=118 (in the reaction with Cf-target). The previous experiments with ^{48}Ca-ions showed that in the region of superheavy elements with Z=112-116 the contribution of the quasi fission (QF) component into the total reaction cross-section σ_{QF}/σ_{cap} is approximately constant and forms more than 90%.

The preliminary results of the experiment show that at the transition from ^{48}Ca to ^{50}Ti-ions the capture cross section σ_{cap}, and hence the fusion-fission cross section σ_{FF} decreases in about 3 times at the E*=45-50 MeV. At the same time, the capture cross-sections σ_{cap} as functions of excitation energy above the Coulomb barrier ($E^*-E^*_B$) are very similar for both reactions. Thus, the spherical neutron magic nucleus ^{50}Ti (N=28) seems to be a promising candidate for the reactions of synthesis of superheavy elements.

In 2006 the final analysis of the experimental data on the study of the fusion-fission and quasi-fission processes for the superheavy nuclei produced in the reactions with ^{48}Ca and ^{58}Fe-ions has been completed. Some new important physical results based on these data were obtained.

1. In the case of the fission process as well as in the case of quasifission, the observed peculiarities of mass and energy distributions of the fragments, the ratio between the fission and quasifission cross sections are determined by the shell structure of the formed fragments.
2. It was observed in the reactions ^{48}Ca,^{58}Fe+^{208}Pb that TKE for quasi-fission process is higher then those for fusion-fission.
3. A further progress in the field of synthesis of superheavy nuclei can be achieved using hot fusion reactions between actinide nuclei and ^{48}Ca ions as well as actinide nuclei and ^{58}Fe ions. Of course, for planning the experiments on the synthesis of superheavy nuclei of up to Z = 122, new research and more precise quantitative data obtained in the processes of fusion-fission and quasifission of these nuclei in reactions with 58Fe-ions are required.
4. Local minima are observed in $<M_\gamma>$ as a function of mass suggesting the great influence of nuclear structure of fission fragments on $<M_\gamma>$. The different dependence of $<M_n>$ and $<M_\gamma>$ as a function of fission fragment mass, total kinetic energy and excitation energy for fusion-fission and quasifission processes were observed.

In 2006, in the framework of the collaboration between the FLNR (JINR) and the Accelerator Laboratory of the University in Jyvaskyla (Finland) and Dipartimento di Scienze Fisiche dell'Università di Napoli (Italy) the experiment devoted to binary fragmentation in the intermediate mass system ^{32}S + ^{100}Mo was carried out[6].

In the binary fragmentation channel of the system ^{32}S + ^{100}Mo at E_{lab} = 160-280 MeV neutron, proton and α-particle multiplicities were measured, as well as the cross section and the Mass-TKE distribution of the fragments. This experiment provides new information on the dynamics of the binary fragmentation in systems with mass A < 150 at low energy for which no data are available. The knowledge

of the binary fragmentation cross section and of the light particle multiplicities allows to put severe constraints on the models used to evaluate such characteristics as time scale, the nuclear deformation and the nuclear viscosity.

The set-up consisted of following parts: the CORSET+HENDES+DEMON +LCP detectors (Fig. 5) from the 8πLP apparatus (LCP – light charged particles).

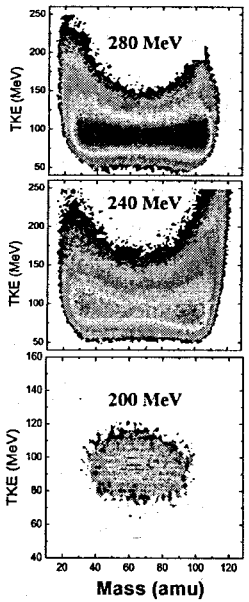

Fig. 5. CORSET+HENDES+DEMON+LCP set-up and the mass-TKE distribution for the binary fragmentation products of the $^{32}S+^{100}Mo$ reaction

Two points of the beam energy were chosen. At each of these energies we measured: 1) Mass-TKE distribution for the binary fragmentation (Fig. 5); 2) energy spectra and angular distributions of neutrons, protons and alpha particles in coincidence with both fragments, in and out of the reaction plane.

Separator VASSILISSA

In the two campaigns using the GABRIELA (Gamma Alpha Beta Recoil Invetsigations with the ELectromagnetic Analyser) set-up [7], the odd isotopes of ^{253,255}No and ^{255}Lr were produced with an intense (~ 0.6 pμA) ^{48}Ca beam impinging on rotating ^{207,208}Pb and ^{209}Bi targets. During the experiments, calibration runs were regularly performed with ^{164}Dy and ^{174}Yb targets to produce well studied Rn and Th isotopes, in particular the well know 181 μs isomeric state in ^{207}Rn to check the calibration of the electron detectors [8].

In the case of the $^{253-255}$No evaporation residues, their implantation in the position sensitive detector is followed mainly by α-decay. In prompt coincidence

with the characteristic α emission of both nuclei, γ quanta as well as conversion electrons were detected in GABRIELA [9].

The analysis of these data as well as the data collected on ^{255}Lr (Fig.6) is still in progress.

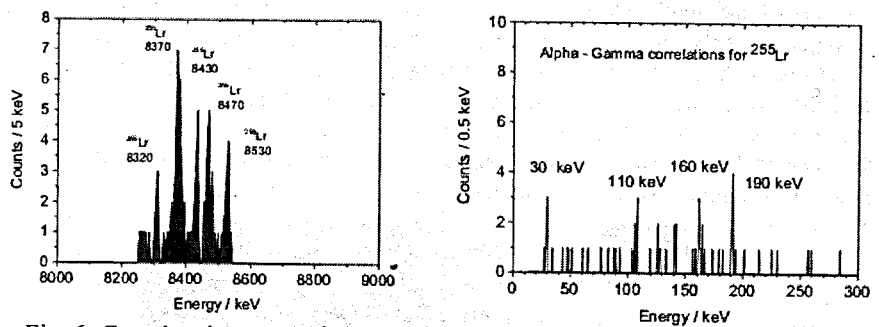

Fig. 6. Correlated spectra of α-particles and γ-quanta from the decay of ^{255}Lw

Modifications to the electronics and focal plane chamber are being performed to increase the efficiency and sensitivity of GABRIELA in view of the next campaign of experiments. In particular, the number of electronic channels for the β detection will be increased in order to increase the efficiently of β coincidences.

Test experiments using high intensity (> 2 pμA) ^{22}Ne beam and ^{208}Pb, ^{209}Bi, ^{238}U targets were performed in the year 2006. It was shown that rather high (~ 5 %) transmission efficiency for slow evaporation residues could be achieved. It means that appropriate statistics for α – γ and α - β coincidences at the focal plane of separator for neutron rich Rf isotopes produced with ^{22}Ne beam and ^{242}Pu target could be collected during one month of the beam time. This experiment has been performed during November 2006. The data acquisition is in progress.

Fragment separator COMBAS

During 2006 year on the in-flight separator COMBAS, ^{11}B (33 AMeV) + ^{12}C (1 mg/cm^2) experiment has been carried out devoted to the production of neutron-rich isotopes with Z = 2-6. Produced experimental data is processing and analyzing.

The multi-detector system from 32 strips Si ΔE-E detectors and CsI/Tl E-detectors has been commissioned and installed in the COMBAS final focal plane to register the coincidences of ^{11}B breakup products. The multi-channel electronics system and the appropriate data acquisition system has been designed and commissioned to satisfy the demand of multi-particle spectroscopy measurements.

Using the Quantum Molecular Dynamics (QMD) model CHIMERA code, the simulations of velocity, isotopic and element distributions of fragmentation products induced in the reactions ^{18}O (35 A·MeV) + ^{9}Be (^{181}Ta) has been implemented and compared with experimental data [10].

Exotic decay modes. 4-π detector FOBOS

In series of experiments using different time-of-flights spectrometers we observed for the first time unusual decay mode of ^{252}Cf (sf) which was treated as "collinear cluster tripartition" (CCT). So far experimental manifestations of this decay channel were obtained in the frame of the "missing mass" method.

It means that only two almost collinear fragments were detected in coincidence and they were much smaller in total mass than initial nucleus. It is reasonable to suppose that "missing" mass corresponds to the mass of undetected fragment (or fragments) flying apart almost along a common fission axis. Shell effects in the resultant fragments seem to be decisive for the process of interest.

Fig. 7. The mini-FOBOS setup at the neutron line 6b of the reactor IBR-2

In the framework of the "missing mass" method fission of $^{236}U^{*}$ produced in the reaction $^{235}U + n_{th}$ has been examined. For this purpose during the year 2006 the mini-FOBOS setup has been installed at the neutron line 6b of the reactor IBR-2 (Fig. 7) and the series of measurements has been performed [11]. The data acquisition is in progress.

High-resolution beam-line ACCULINNA

Experiments aimed at the search for an ultra exotic nucleus ^{7}H which could be produced in the reaction ^{2}H(^{8}He,^{3}He)^{7}H. The setup employed in these experiments is outlined in Fig. 8. It was designed taking into consideration a possibility to furnish information characterizing another nucleus – ^{9}He. Results obtained in these experiments were analyzed in 2006 [12].

Result obtained on the ^{7}H nucleus. Earlier, we revisited the long-standing issue of the ^{7}H nucleus setting an upper limit of 3 nb/sr for the cross section of the reaction ^{2}H(^{8}He,^{3}He)^{7}H which could populate a quasi stable ($T_{1/2}\geq 1$ ns) resonance state in ^{7}H. Based on the energy and width of the ground-state ^{5}H resonance, one makes sure that, being found, this hypothetical nucleus will undergoes a unique, five-body decay. Most likely the ^{7}H reveal itself as a narrow resonance ($\Gamma<0.5$ MeV) observed at energy $E<2$ MeV above the ^{3}H+n+n+n decay threshold.

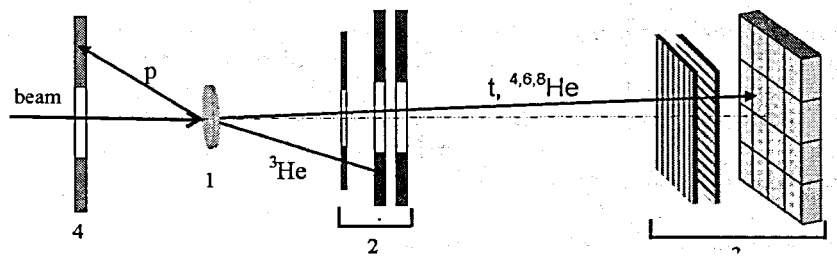

Fig. 8. Schematic diagram showing the assembly of the target and detector array employed in the experiments. 1 – deuterium target; 2 – annular detector telescope destined for ^{3}He nuclei emitted in the ^{2}H(^{8}He,^{3}He)^{7}H reaction; 3 – detector array (a pair of Si strip detectors backed with a wall built of CsI(Tl) counters) for tritons and helium nuclei; 4 – annular Si strip detector for protons resulting from the ^{2}H(^{8}He,p)^{9}He reaction.

A 25 MeV/nucleon beam of ^{8}He ions obtained from the ACCULINNA separator bombarded a cryogenic target cell filled with deuterium gas. A telescope consisting of three annular silicon detectors (telescope 2 in Fig. 8) was intended for finding ^{3}He nuclei escaping from the deuterium gas target. The energy and emission angles measured for the ^{3}He nuclei were used for finding the ^{7}H energy done with the use of the missing mass method. The forward-angle telescope included in the setup (telescope 3 in Fig. 8) provided the detection of tritons emitted at the ^{7}H decay. By requiring that the ^{3}He nuclei are detected in coincidence with these tritons one could be eliminate some part of background.

Helium-3 nuclei moving in forward direction were detected in coincidence with tritons emitted in the ^{7}H resonance decay (see Fig. 8). All particles detected by these telescopes, and also the ^{3}He and ^{3}H nuclei, were identified by their positions in the ΔE×E plot. The geometry of this setup was optimized for the study of the ^{2}H(^{8}He,^{3}He)^{7}H reaction in a range of 9 – 21 degrees in the centre-of-mass (CM) system. Energy resolution achieved for the ^{7}H missing mass energy was estimated by Monte-Carlo (MC) simulation taking into account all experimental details. It was found to be 0.6 MeV (FWHM).

After two weeks of continuous bombardments a total flux of 2×10^{10} was achieved for ^{8}He nuclei passing through the deuterium target. A ^{7}H missing mass spectrum resulting from the detected ^{3}He-^{3}H coincidence events is presented in Fig. 9, panel B. Panel A in Fig. 9 shows the ^{7}H spectrum derived from the data collected for single ^{3}He nuclei. Evidently, the richer pattern seen in the spectrum of panel A was due to the huge number of ^{4}He nuclei detected by telescope 2. The tail of the ^{4}He locus could fall partly into the ^{3}H locus in the ΔE×E plot. From the few events observed in the spectrum of Fig. 9, panel B, only a cross section limit $d\sigma/d\Omega\leq 20$ μb/sr follows for the reaction ^{2}H(^{8}He,^{3}He)^{7}H populating a resonance lying between 0 and 3 MeV above the ^{7}H decay threshold.

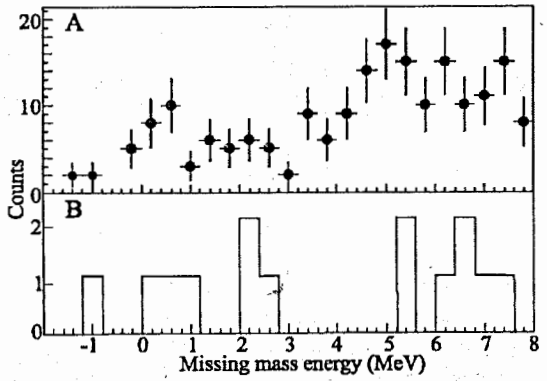

Fig. 9. Missing mass spectrum of the ^{7}H nucleus derived from the data of the ^{2}H(^{8}He,^{3}He)^{7}H reaction. **A** – the spectrum obtained from the data on the single ^{3}He nuclei, **B** – the spectrum obtained from the analysis of ^{3}He-^{3}H coincidence events.

New insights into the low-energy ^{9}He spectrum. ^{9}He nucleus has been produced in the one-neutron transfer reaction ^{2}H(^{8}He,p)^{9}He [13]. This "classical" (d,p) reaction is known as a good tool to populate single particle states. Our setup shown in Fig. 8 provided complete kinematical measurements for this reaction. This possibility was foreseen in order to reveal a low-energy s-wave state. Also, we bore in mind that similar correlation measurements allowing us to arrive at clear conclusions about the low-energy spectrum of the ^{5}H nucleus.

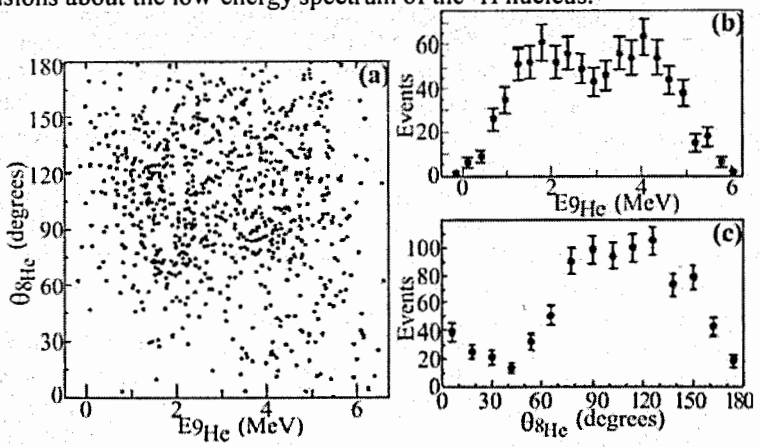

Fig. 10. Experimental data obtained in the study of the ^{9}He nucleus produced in the ^{2}H(^{8}He,p)^{9}He reaction. Shown in panel **(a)** is a correlation plot θ_{8He} *vs.* E_{9He}. The missing mass energy E_{9He} is defined in reference to the decay threshold of ^{9}He; θ_{8He} is the angle between the ^{9}He momentum vector, defined for lab system, and the decay direction of ^{9}He defined for its CM. The two linear spectra shown in panels **(b)** and **(c)** are just the projections of the data of panel **(a)** made on its axes.

Results obtained in the experiment are shown in Fig 10. The total number of ^{9}He events presented in this figure corresponds to a total cross section value of σ=7 mb/sr estimated for the ^{2}H(^{8}He,p)^{9}He reaction. This value is consistent with estimations made for a direct one-neutron transfer mechanism implied for this reaction . Near the threshold, the ^{9}He spectrum exhibits behavior consistent with s-wave and inconsistent with a pure p-wave. This is an indication for a virtual state in ^{9}He.

An important feature of the data is a prominent forward-backward asymmetry with ^{8}He flying preferably in the backward direction in the ^{9}He CM system. To describe such an asymmetry the interference of opposite parity states is unavoidable.

Analysis made for the θ_{8He} distributions taken in different bins of the ^{9}He energy E_{9He} led us to the following conclusion about the three low-energy states of ^{9}He. The lowest resonant state of ^{9}He is found at about 2 MeV with a width of ~2 MeV and is identified as $1/2^{-}$. The observed angular correlation pattern is uniquely explained by the interference of the $1/2^{-}$ resonance with a virtual state $1/2^{+}$ (a limit on the scattering length is given as $a>-20$ fm) and with a $5/2^{-}$resonance at energy $\geq$4.2 MeV.

The θ_{8He} distributions in different bins of ^{9}He energy provide strong evidence that any narrow $p_{1/2}$ state is not populated in the reaction. No matter how weakly the narrow resonance is populated, a close to π value is added to the phase of the $p_{1/2}$ continuum when the ^{9}He energy changes across this resonance. But for all that, the θ_{8He} angular distribution, caused by the $s_{1/2}$–$p_{1/2}$ interference, should change drastically within the energy corresponding to the small width of this narrow resonance. No trend of this kind is observed in Fig. 10. The phase of the broad $1/2^{-}$ state changes slowly and, according to our calculations, the phase shift hardly achieves π in its value. This explains the smooth behavior of the angular asymmetry seen up to E_{9He}=3 MeV in Fig. 10a.

Reactions induced by stable and radioactive ion beams of light elements

At the accelerator complex for radioactive beams DRIBs, experiments were performed with a ^{6}He-beam of about 60 MeV and intensity ~$1\cdot10^{7}$ pps to measure excitation functions of fusion and transfer reactions down to energies around the Coulomb barrier. [14]

^{6}He belongs to the type of light exotic nuclei with a neutron halo – it is regarded as composed of two valence neutrons and a compact α-particle core. This unusual structure is expected to manifest itself in the interaction with other nuclei as an increase of the total reaction cross section, an enhancement of the cross section of complete fusion reactions at sub-barrier energies and an increase in the cross section of neutron transfer reactions, etc.

In 2006 excitation functions were obtained for the fusion reaction ^{197}Au(^{6}He,*x*n)$^{203-xn}$Tl with the consequent evaporation of *x* neutrons in a wide energy range, including deep sub-Coulomb barrier energies. The excitation function of the reaction ^{206}Pb(^{6}He,2*n*)^{210}Po was also measured [15]. From the

obtained results it follows that in the interaction of ^{6}He with Pb and Au a significant enhancement of fusion takes place at energies below the barrier (see Fig. 11 and 12). Such an enhancement is explained by the peculiar structure of ^{6}He, which allows consecutive capture of the two halo neutrons and then of the residue (^{4}He) to for, a compound nucleus.

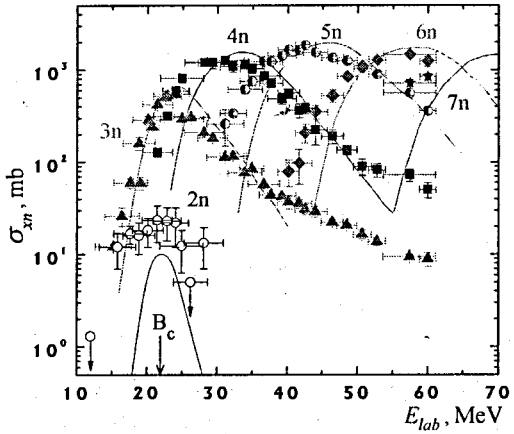

Fig. 11. Experimental excitation functions for the ^{197}Au + ^{6}He → $^{203\text{-}xn}$Tl reaction, where x = 2-7. The symbols denote: ○ – 2n, ▲ – 3n, ■ – 4n, ◐ – 5n, ◆ – 6n, ★ – 7n evaporation channels; the curves – calculations with the statistical "ALICE-MP" code. B_c is the Coulomb barrier for the ^{6}He + ^{197}Au reaction.

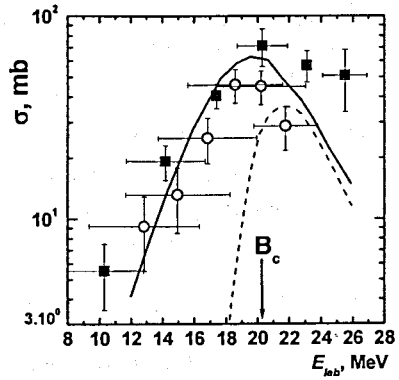

Fig. 12. Excitation function measured for the ^{206}Pb(^{6}He,2n)^{210}Po reaction. ○, ■ denote experimental cross sections for the formation of ^{210}Po from two experiments, dashed line – calculations within the framework of the statistical model, solid line – calculations using the two-step fusion mode, taking into account the beam energy spread.

The excitation functions for neutron transfer in the reaction ^{6}He + ^{197}Au with the formation of the isotopes ^{196}Au and ^{198}Au in their ground states were also measured (Fig. 13). The results of the reaction ^{6}He + ^{197}Au were compared with those of the reaction ^{4}He + ^{197}Au.

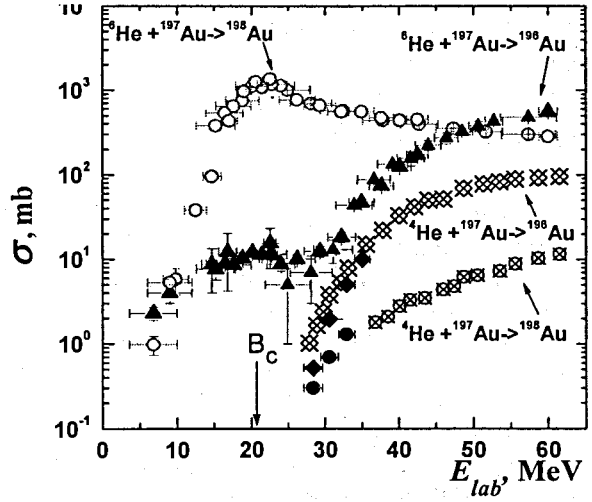

Fig. 13. Experimental excitation functions for the formation of the isotopes ^{196}Au and ^{198}Au. Circles and triangles are for ^{6}He, diamonds and crossed-circles – for ^{4}He.

The excitation functions for ^{198}Au strongly differ. Increasing the incident energy to the Coulpmb barrier, the cross section rises up to about 1.2 b. The behaviour of the cross section of ^{196}Au at sub-barrier energies is also interesting – this can be due to inelastic excitations of the target nucleus with the subsequent evaporation of neutrons. All the obtained data are manifestation of the particular properties of the halo nucleus ^{6}He and hence of its interaction with the target nuclei at energies close to the Coulomb barrier.

The results at sub-barrier energies were confirmed in measurements with high energy resolution using the magnetic spectrometer MSP-144. In the experiments the focusing and the monitoring of the beam was performed with a wide-aperture multi-wire proportional chamber, designed jointly with the Yerevan Physical Institute. It allows registering reaction products with high position resolution and at high intensity (up to 10^6 pps).

Collinear laser spectroscopy

Experiments on the ScII transition 3d4s $^3D_2$ → 3d4p $^3F_3$ at $\lambda \approx 363.1$ nm were performed on the $^{42\text{-}46}$Sc isotopic chain using an ion guide isotope separator with a cooler-buncher. Isotope and isomer shifts and hyperfine structures of five ground states and two isomers were measured. Results on the nuclear moments and charge radii changes were also deduced. The results for the magnetic dipole and electric

quadrupole moments of ^{43,44,44m,46}Sc isotopes were obtained with overall greater accuracy compared to the known data from the literature. The nuclear moments $\mu(^{45m}Sc) = +0.368(5)\ \mu_N$ and $Q_s(^{45m}Sc) = +0.318(22)$ b of ^{45m}Sc are deduced for the first time. The unusually large quadrupole moment of the isomeric state of ^{45m}Sc is the most striking feature of the present data. It leads to a larger charge radius of the isomeric state than follows from the isotope shift. This surprising fact remains so far unexplained.

Theoretical and computational physics

Damped collisions of tranactinide nuclei ($^{238}U+^{238}U$, $^{232}Th+^{250}Cf$ and $^{238}U+^{248}Cm$) have been studied in detail [16] within the realistic model based on solution of multidimensional transport equations. Large charge and mass transfer was found in these reactions due to the inverse (anti-symmetrizing) quasi-fission process leading to formation of survived superheavy long-lived neutron-rich nuclei, suitable for subsequent chemical analysis. Lifetime of the composite system consisting of two touching nuclei (giant quasi-atoms) was found to be rather long; sufficient for spontaneous positron formation from super-strong electric field, a fundamental QED process not observed yet.

Fusion-fission process in the superheavy mass region was studied by solving the time evolution of nuclear shape in three-dimensional deformation space using the Langevin equations. The critical area was identified where the trajectory's destination is determined to be the fusion or the quasi-fission process [17]. Neutron emission in fusion-fission process was also studied on the basis of the fluctuation-dissipation model combined with a statistical model. The structure of the distribution of pre-scission neutron multiplicity depending on incident energy was investigated.

Within the recently found mechanism of sequential neutron rearrangement with a positive Q-value a huge enhancement of sub-barrier fusion of weakly bound nuclei was predicted and a new experiment was proposed for measuring and comparing the evaporation residue cross sections in the $^{6}He+^{206}Pb$ and $^{4}He+^{208}Pb$ reactions leading to the same compound nucleus. The yield of polonium isotopes at the same sub-barrier center-of-mass energy of 15 MeV (5 MeV below the barrier) was predicted to be three orders of magnitude larger for the first reaction as compared to the second one [18]. This experiment has been performed recently in Dubna and the obtained results agree well with the predictions.

The knowledge base on low energy nuclear physics, "Nuclear Reactions Video", allocated at the Web-site http://nrv.jinr.ru/nrv, was significantly extended and improved [19]. Several new computational codes on low-energy nuclear dynamics (nucleon transfer, multidimensional double-folding potential energy surface, adiabatic two-center shell model) have been included into the knowledge base. The digital databases on fusion reactions and yields of evaporation residues have been filled with several hundreds experimental cross sections. All the resources of the knowledge base are available on-line via the standard Web browsers using CGI technology and Java applets.

Heavy ion interaction with matter

The study of surface sputtering processes in constructive materials in dependence on the specific energy loss of heavy ions and damage dose level has been continued. Atomic force microscopy studies of nanoscale structural defects on the surface of single crystalline Al_2O_3, ZrO_2:Y and $MgAl_2O_4$, irradiated with krypton, xenon and bismuth ions are underway. The systematization of experimental data on geometrical parameters of defects formed by single heavy ions as a function of electronic stopping power has been continued.

Track membranes and the modification of polymers

Investigations of the process of etching of micro- and nano-pores in ion-irradiated polymers, with the use of surfactant-enhanced etchants, have been in further progress. Nanopores of a special shape produced this way have been applied for the first time to build a pinhole camera for atomic nanolithography. Image of a template object is obtained at a reduction of 1:8000 and a resolution of 50 nm.

In the framework of this activity, a new method for production of track membranes with high through-put and high selectivity has been suggested. The method implies that both the pore diameter and pore density change across the membrane thickness. Membranes with such structure have shown high performance. Russian patent application has been submitted.

In collaboration with the Institute of Crystallography of RAS, research work on chemical modification of PET track membranes have been performed with the aim to reduce sorption losses when filtering biological preparations. Using modification with polyethyleneglycols, the sorption has been reduced by tens times.

A procedure of preparation of micro- and nanostructural materials (nanowires, nanotubules as well as nanomembranes with a selective layer) on a basis of polymeric compositions with nonlinear-optical properties with application as matrices of poly(ethylene terephthalate) track membranes has been developed. The laws of formation of these materials and their structural properties were investigated. To produce the polymeric nanomaterials, a flushing method was used. It is shown that varying the parameters of the process of deposition of copolymers on the track membranes surface provides a way for producing a big assortment of composite nanomembranes with a selective layer as well as nanowires and nanotubules with a wide spectrum of characteristics.

Radioecological research, production of ultrapure radioisotopes

The studies are performing to improve the radiation control in the environment and the technological safety in nuclear plants, to develop the novel technologies of the radioactive materials treatment, to apply nuclear methods in nuclear medicine (diagnostic and therapy) with using following isotopes: ^{67}Cu, ^{73}As, ^{88}Zr, ^{99}Mo(^{99}Tc), ^{97}Ru, ^{149}Tb, ^{178}W(^{178}Ta), ^{186}Re, ^{188}Re, ^{211}At, ^{225}Ac, ^{237}U, ^{236}Pu, ^{237}Pu.

The special attention was given to development of methods of radioisotopes producing in (α, xn) reactions on cyclotron U-200 and in photonuclear reactions on microthrone MT-25.

Physics and heavy ion accelerator techniques

U400 cyclotron

In 2006 the U400 cyclotron was mainly used for the experiments with $_{48}Ca^{5+}$ ions for the synthesis of superheavy elements. The further modernization of the U400 axial injection gave the possibility of increasing the $^{48}Ca^{+5}$ current into the injection line from 40÷60 to 80÷100 μA. Correspondingly, the average output $^{48}Ca^{+18}$ ion current was increased from 15 to 25 μA. A diagram of the U-400 operation in 2006 is shown in Fig. 13. This year the following ions were accelerated: $^{6}Li^{1+}$, $^{22}Ne^{3+}$, $^{40}Ar^{4+}$, $^{48}Ca^{5+}$, $^{58}Fe^{6+}$, $^{84}Kr^{8+}$. The overall efficiency (total beam time/beam on target) was close to 95 %.

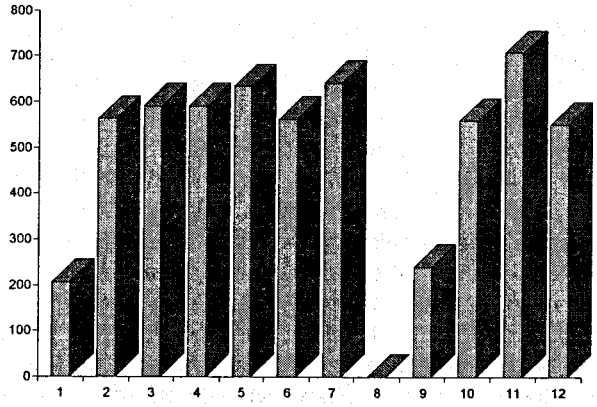

Fig. 13 Operation time of U400 in 2006.

U400M cyclotron

The accelerated ions were $^{7}Li^{+2}$, $^{11}B^{+3}$, $^{20}Ne^{+7}$. Operation time as injector for the DRIB's romplex was 1100 h (30 %) The overall efficiency was close to 90 %.

The modernization of U400 is planned during 2007 for the improvement of the cyclotron parameters. The aims of the modernization were:

- to increase the light ion beams intensity by the factor of 4 – 5 for producing of secondary beams,
- to improve the quality of beams,
- to increase the maximal energy of accelerated ions up to 100 MeV/A,
- to improve the radiation safety conditions,
- to accelerate "low" (6÷15 MeV/A) energy ions (move some experiments from U400 to U400M),
- to extract the beams to the second direction.

Design of accelerator complexes for condensed matter physics and nuclear medicine.

A creation of the specialized accelerating complexes for condensed matter investigations and nuclear medicine was continued. The first such complex on the basis of cyclotron DC-60 (Fig. 13) has been launched at L.N. Gumilev Euroasia State University in Astana (Kazakhstan) in 2006.

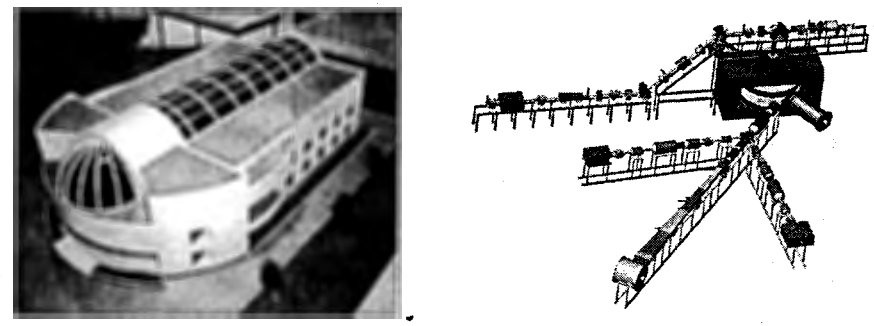

Fig. 13. DC60 cyclotron for the Research Center at the L.N. Gumilev Euroasia State University in Astana (Kazakhstan)

Development of nuclear-medical researches demands creation of multi-purpose accelerators with beam of protons and heavy ions providing producing of isotopes for diagnostics and therapy and beam therapies. The construction of the first accelerator DC-72 for the Cyclotron Center of Republic of Slovakia will be completed in 2007.

References

[1] Yu.Ts. Oganessian *et al., Phys. Rev. C* **74**, 044602 (2006).
[2] Yu.Ts. Oganessian *et al.*, submitted to *Phys. Rev. C.*
[3] S.N. Dmitriev *et al., Int. Symp. on Exotic Nuclei "EXON2006"*, Khanty-Mansiysk, Russia, 17-24 July, 2006.
[4] R. Eichler *et al.*, submitted to *Nature.*
[5] M. G. Itkis *et al.*, to be published in Int. *J. of Modern Phys. E.*
[6] E.M.Kozulin *et al.*, To be published in *Am. Inst. of Phys. (AIP)*
[7] A. G. Popeko *et al., Phys. of At. Nucl.* **69**, 1183 (2006)
[8] K. Hauschild *et al., Nucl. Instr. & Meth. A* **560**, 388 (2006).
[9] A. Lopez-Martens *et. al., Phys. Rev. C* **74**, 044303 (2006).
[10] A.G. Artukh *et al., Acta Phys. Pol. B*, 6, 1875 (2006).
[11] D.V. Kamanin *et al.*, to be published in *Phys. of At. Nucl.*.
[12] M.S. Golovkov *et al.*, submitted to *Phys. Rev. C.*
[13] G.M. Ner-Akopian *et al.*, to be published in *Eur. Phys. J.*
[14] Yu.E. Penionzhkevich *et al.*, Submitted to *Eur. Phys. J. A.*
[15] A.A. Kulko *et al.*, to be published in *Physics of Atomic Nuclei.*
[16] V.I.Zagrebaev *et al. Phys. Rev.* **C73**, 031602(R) (2006).
[17] Y. Aritomo and M. Ohta, *Nucl. Phys.* **A764**, 149 (2006).
[18] Yu.E. Penionzhkevich et al., Phys. Rev. Lett. **96**, 162701 (2006).
[19] V.I. Zagrebaev et al., http://nrv.jinr.ru/nrv